Potential of Formation Flight for Commercial Aviation: Three Case Studies

Thomas E. Kent* and Arthur G. Richards†
University of Bristol, Bristol, England BS81TR, United Kingdom

https://doi.org/10.2514/1.C035954

Formation flight has the potential to significantly reduce aircraft fuel consumption by allowing "follower" aircraft to fly in the aerodynamic wake of "leader" aircraft. However, this requirement for aircraft to be in close proximity for large parts of their journey raises questions about the suitability of flying in formation given the diverse range of existing flights and geographical regions. This paper demonstrates the potential for two-aircraft formation flight for three distinct case studies: long-haul airline, transatlantic airline, and low-cost airline, encompassing a range of typical airline regions and characteristics. The results indicate, even with only minor scheduling alterations, the potential fuel savings could result in saving hundreds of millions of dollars in fuel costs and reducing millions of tonnes of carbon dioxide emissions. An analytical geometric method for calculating all possible combinations of optimal routes is presented. This is coupled with a mixed integer linear program for providing an assignment of aircraft into formation pairs. A number of different key metrics, correlations, and predictive indicators help to determine which flights, airlines, and regions show "good" formation potential. Importantly, this paper also demonstrates these results for a wide range of drag-reduction possibilities and the impact this has on achievable fuel saving.

I. Introduction

REPORTS [1,2] estimate passenger numbers are estimated to surpass eight billion by 2037 with continuing growth in passenger demand for air transport maintaining historic levels of between 5 and 6% per year. Therefore, commercial aviation is constantly looking for ways to cope with these increases in demand [3,4] while reducing costs. Furthermore, there is an ever mounting need to look for ways to mitigate the resulting impact this increase in passengers has on the environment [5,6]. Therefore, the focus of much of modern aviation-related research aims to address these issues by making air travel cheaper, more efficient, and significantly more environmentally friendly. It is clear that in order to achieve such environmental goals [7], without radical changes to current aircraft fleets, breakthroughs of operational concepts are required. The work of this paper looks at one potential concept for commercial aviation: formation flight.

One of the immediate benefits of formation flight, over other proposed fuel-saving methods such as air-to-air refueling or blended-wing/body aircraft [8,9], is the relatively minimal change to the current airframes. The majority of today's commercial airliners can fundamentally observe a reduction in drag from formation flight [10]. The most immediate changes required would be from the areas of air traffic management and avionics; however, these challenges should not be underestimated.

Formation flight has long been used within the military to provide an effective approach for safely moving large numbers of aircraft [11]. However, flying in close proximity (in particular, in the *wake vortices* [12,13] of other aircraft) can also be used to obtain a drag reduction. Therefore it is of great interest to see how formation flight can be used to reduce fuel burn within commercial aviation. Before formation flight can become a realistic fuel-saving method for commercial aviation, a number of key areas must first be addressed. These include, but are not limited to, aerodynamics and simulation [10,14–24]; control and automation [12,15,19,25–27]; routing and assignment [21,28–30]; and operations and regulations [1,4].

Flight tests, aerodynamic simulations, and analytical study help to show the potential for formation flight from the microlevel of a particular single formation setting, but few look at the larger *fleet-level* (or macrolevel) problem of assigning aircraft into those formations. Works by Blake and Multhopp [14], Blake and Gingras [15], Jacques et al. [16], Wagner et al. [17], Vachon et al. [18], and Ray et al. [19] all showed significant induced-drag-reduction figures for two aircraft flying in formation, ranging from 25 to 59% and resulting in fuel-flow reductions of between 8 and 18%. These numbers help to estimate formation drag-reduction values used within this paper. Furthermore, the works of Ribichini and Frozzoli [31] and, more recently, Bower et al. [10] and Xu et al. [20,21] use these drag-reduction values to demonstrate promising results for real world flights. However, aerodynamic simulations by Ning et al. [32] and range-equation estimates by Voskuijl [24] conclude that to reach higher savings, aircraft would need to reduce their Mach number by roughly 2% and fly at a slightly higher altitude. Crucially for the commercial flight setting, Ning et al. [13,32] have demonstrated that even in "extended formation flight," where aircraft can be separated longitudinally by 10–40 wingspans, these fuel savings are possible.

However, assuming an aerodynamic benefit of flying in the wake of another aircraft, it is still essential to be able to predict and track both the evolution of the wake vortices left by aircraft [12,27] and the aircraft itself [13] while maintaining a position relative to them [33,34]. Demonstrating the importance of tracking the optimal region of drag reduction, Zhang and Liu [26] show that to maintain at least 90% of the maximum drag reduction, the so-called sweet spot has to be tracked within 5% of a wingspan. DeVries and Paley [12,27] explore the need be able to simultaneously track the wake of lead aircraft and control the follower aircraft's position. Formation-hold autopilots have also been introduced to enable formations to stay in position relative to each other [25,35,36].

While flight tests and aerodynamics are a motivation, the process of modeling, predicting, and measuring the benefits and practicalities are not explored in this paper. Instead, these topics are assumed to be sufficiently solvable to allow for formation flight to occur and instead help to estimate feasible drag reductions. Each of the aforementioned form core research areas and will contribute to the overall success of commercial formation flight; the work of this paper is focused on assessing the *routing and assignment problem*.

Seminal work on the coupled formation routing and assignment problem was introduced by Ribichini and Frozzoli [31]. Optimal routes comprise great circle paths, ignoring wind, and assume per-unit

Received 25 March 2020; revision received 17 July 2020; accepted for publication 18 August 2020; published online 25 November 2020.

*Research Associate, Department of Computer Science, Queens Building. Student Member AIAA.

†Professor in Dynamics and Control, Department of Engineering, Queens Building. Senior Member AIAA.

distance fuel reductions of 10 and 15% when flying in formations of two and three, respectively. An example three-flight study resulted in overall savings of 9.2% against solo flight. The work also implements a "proposal–marriage"-type greedy algorithm for decentralized assignment of flights into formations, outlining their concerns with tractability of the larger globally optimal problem. The work of Bower et al. [10] improved upon the basic routing methods with a focus on aerodynamic performance and formation geometries. In addition to the aerodynamic approach, the authors outline a small case study for five FedEx flights, creating a formation of two and one formation of three, resulting in fuel savings of 7.8 and 12.5%.

The work by Xu et al. [20,21] combines route optimization, an aerodynamic model by Ning et al. [13], and an assignment optimization. To try to mitigate the massively combinatorial problem of assigning aircraft into formations, which we refer to as the *global assignment problem*, a heuristic approach of preemptively discarding "bad" formations is used. A smaller subset of remaining possible candidate solutions is then optimized for formation flight. A gradient-based optimization is used to calculate values for a number of design variables, such as rendezvous locations and altitudes, and provides reasonably high-fidelity solutions that include a schedule optimization. The results presented are based on their Star Alliance case-study of 150 transatlantic flights, and show extremely promising overall savings of 7.7%, even with scheduling constraints. However, the extent of the computational time required (roughly 200 h for 2500 formation combinations) shows the need for a faster approach if the larger global assignment problem is to be assessed.

For formation flight to become a reality within the commercial flight sector, significant potential needs to be shown. It is therefore necessary to investigate a number of differing scenarios where formation flight may be of benefit. This paper presents a comparison of three distinct datasets to assess its feasibility, with the objective of observing patterns and influencing factors affecting formations and the associated fuel savings. Importantly, all of the results of this paper will focus on formations with a size of two (i.e., pairs); however, for larger formations, analogous methods have been addressed previously by Kent [37].

We will first, in Sec. II, review the use of a geometric approach to calculate routes for two-aircraft formations, coupled with the use of an optimization to assign individual aircraft into formation pairs. The key feature of this approach is the ability to assess a very large number (hundreds of thousands) of potential formations in a short amount of time. Three case studies, each with a set of flights with potential for using formation flight, will be introduced in Sec. III, along with an attempt to categorize them using a simple graph-theoretic approach. The results of applying the methodology of Sec. II to each of the case studies will then be discussed in the remaining Secs. IV–VI. The aim is to study the sensitivity of changes at the micro level (individual formation), such as rates of fuel burn during formation flight or restrictions on scheduling, in order to observe the effect this has on the results of the macrolevel (global fleet assignment).

Initially, in Sec. IV, we outline solutions for a baseline 10% formation fuel-saving factor, where we will present the impact schedule restrictions have on performance. With those, in Sec. V, we look at a metric for quantifying formation flight potential and possible predictive indicators of characteristics that lead to "better performing" formations. Finally, in Sec. VI, the impact of the formation fuel-saving factor is investigated, examining results for formation discount factors between 1 and 20%.

II. Geometric Approach to Optimal Formation Routing and Fleet Assignment

The core methodology outlined in this section is directly taken from the authors' previous works of Refs. [29,37]. For brevity, an overview of the geometric method will be presented here. The key focus behind the method is to enable rapid calculations, in just a few milliseconds per formation, of the optimal formation routes by using an analytic, geometric method. In this paper, we choose to limit formations to two aircraft; however, in Sec. II.C, we discuss how the following methods can extend to formations of three or more.

To introduce the route optimization method, begin by assuming aircraft only at cruise at a constant altitude, and with constant rates of fuel burn per unit distance. Two flights, flight A and flight B, fly from two distinct origins, A and B, to a common destination C. Under the assumptions, the optimal flight will consist of two solo straight-line legs, from A and B, respectively, to a common join point P, and then a shared leg from P to the destination airport C. The formation routing problem is then defined as finding the point P joining A, B, and C together such that the sum of the fuel burned is minimized. Extensions to allow for differential fuel-burn rates, along with the removal of a number of simplifying assumptions, are discussed in Sec. II.C.

A. Using Arc Weights to Represent Formation Flight

To incorporate the concept of benefiting from drag-reduction from flying in formation, a notion of "arc weighting" will be used. An arc represents a flight between two points, such as a solo flight from A to C or a formation leg from P to C. The relative "cost" (in this case, the cost in fuel burned) of each arc can be formulated by adding weightings. This fuel-burn constant is used as the arc weightings for each flight, to take into account distinct aircraft types and corresponding differing rates of fuel burn. EUROCONTROL'S Base of Aircraft Data (BADA) [38] can provide estimates to the fuel-burn rates.

The proportion of fuel used along the formation arc of the flight should, however, be less than if the aircraft were not in formation. The control and distribution of the formation (e.g., leader selection) is assumed to be determined separately, and only an aggregate fuel-burn rate for the whole formation is used for route optimization. Ideally, this would be based on a detailed consideration of the aircraft types involved. However, this is beyond the scope of this paper. For the purposes of this work, for a formation size of two, a nominal formation fuel-burn factor (denoted λ_f) of 0.9 is used initially, based on estimates from the results of Refs. [14,15,23,28,29,37,39–41]. That is, if the front aircraft receives no saving while the follower saves 20%, the resulting average is taken to be $(1 + 0.8)/2 = 0.9 = \lambda_f$ relative to both aircraft in solo flight. The method will readily extend to a more detailed determination of this factor based on formations of particular types of aircraft. In terms of scalar arc weighting, this means that at the formation stage of the flight, each member contributes the proportion λ_f (e.g., 0.9) of their own weighting and the total estimated fuel burn per unit distance on the formation arc is simply the sum of all these contributions. In Sec. VI, we will look more closely at the impact the value λ_f has on potential fuel saving.

Take flight A and flight B, that each depart from airports A and B and have a single shared destination airport C, but want to join in formation via a point P. As shown in Fig. 1, let the solo arcs AP and BP have arc weightings of w_A and w_B, respectively (taken from BADA). The weight of the formation arc PC is $w_C = (w_A + w_B) \times 0.9$. With this in mind, the problem is then to find the optimal location for this point P. This can be considered the "microproblem" of trying to find the optimal route for two aircraft in order to fly in formation. The following looks to use an adaptation of the Fermat point problem to solve this.

B. Basic Geometric Method

The approach is based upon the Fermat point problem [42,43]: given triangle ABC on the Euclidean plane, find a point P such that the sum of the distances $\|\boldsymbol{PA}\|$, $\|\boldsymbol{PB}\|$, and $\|\boldsymbol{PC}\|$ is minimized. The problem can be extended to include the notion of weighted arcs, allowing the representation of differing costs per unit distance. For the three vertices A, B, and C and the join point P, the scalar weights w_A, w_B, and w_C correspond to the arcs PA, PB, and PC, respectively

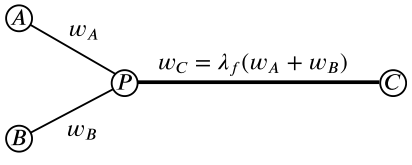

Fig. 1 Arc weightings representing formation flight.

(shown in Fig. 1). The problem is then minimizing the sum of the weighted vectors normalized by their distances:

$$f(P) = w_A \frac{\boldsymbol{PA}}{\|\boldsymbol{PA}\|} + w_B \frac{\boldsymbol{PB}}{\|\boldsymbol{PB}\|} + w_C \frac{\boldsymbol{PC}}{\|\boldsymbol{PC}\|} \tag{1}$$

From the minimal energy principle [42], this system has an equilibrium point when $f(P) = 0$, and so the location of P is chosen to achieve this equilibrium. From the law of cosines, this leads to expressions θ_A, θ_B, and θ_C for the intersection angles $\angle BPC$, $\angle APC$, and $\angle APB$, respectively (as in Fig. 2):

$$\theta_A = \cos^{-1}\left(\frac{w_A^2 - w_B^2 - w_C^2}{2w_B w_C}\right), \qquad \theta_B = \cos^{-1}\left(\frac{w_B^2 - w_A^2 - w_C^2}{2w_A w_C}\right),$$
$$\theta_C = \cos^{-1}\left(\frac{w_C^2 - w_A^2 - w_B^2}{2w_A w_B}\right) \tag{2}$$

It is important to note that these expressions are obtained solely from the input of the three scalar weight values w_A, w_B and w_C, and are therefore independent of any physical location [42].

Knowing these three angles eliminates the need for a fixed destination vertex C. Two fixed points A and B and a formation angle θ_C, at which the trajectories must meet, inscribe two circles that define the loci of possible formation points (as shown in Fig. 3) for all possible destinations.

Therefore, given any pair of nodes $\{A, B\}$ with three arc weights w_A, w_B, and w_C, the two inscribed circles (each with a "back vertex" X) can be constructed. Then, for any destination C, the formation join point must lie at the intersection of the line CX and the locus arc of possible join points (at most, only one of the back vertices will be used, with the choice depending on the location of the destination node).

When routes have distinct departure and arrival nodes, then this approach must be applied to both "ends"; thus, the problem is to find both a rendezvous location and the point at which a formation should break away. This construction is depicted in Fig. 4 for two solo routes between AC and BD (the black lines). First, the circles and back vertices are calculated for each pair $\{A, B\}$ and $\{C, D\}$. Then, the arc joining a back vertex X_i of $\{A, B\}$ to a back vertex Y_j of $\{C, D\}$ $(i, j \in \{1, 2\})$ should cross both circles at the required angles (the dotted black line). This results in two crossing points, P and Q, which are the respective join and break points of the formation. However, if no single arc exists that satisfies the angles of Eq. (2) on both circles, then the optimal path is the shortest path between either X_i and C or D, or Y_i and A or B so that the angles are satisfied only once. If that is not possible, then the formation arc will simply connect A or B to either C or D. The resulting route flown for each aircraft is then $A \to P \to Q \to C$ and $B \to P \to Q \to D$.

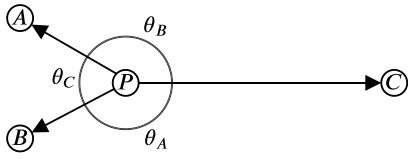

Fig. 2 Three-point vectorial representation and corresponding angles.

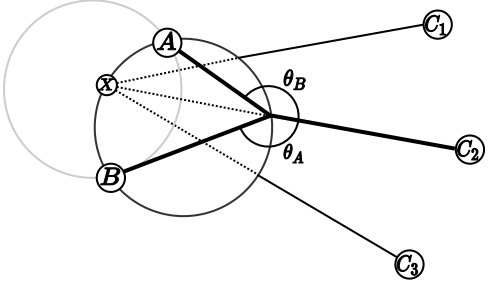

Fig. 3 Possible solution points given an angle of interception.

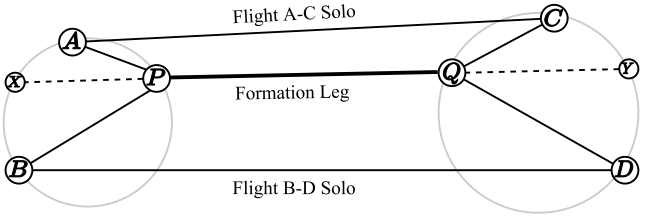

Fig. 4 Geometric construction of optimal formation rendezvous point *P* and breakaway point *Q*.

C. Additional Extensions of the Geometric Method

The key methods of the geometric routing approach have been outlined; however, a number of important additional extensions have been explored in detail by the authors in [29,37]. First, while the methods of this section are inherently planar, they can be easily extended to work on the surface on a sphere; importantly, this enables the use of great circle paths. Second, a notion of a minimum distance required to climb and descend allows the inclusions of radial constraints around each of the airports, ensuring flights have room to either climb to their required cruise altitudes or descend from them. Additionally, this framework allows the routing problem to be decoupled, reducing pairs of nodes to their back vertices and inscribed circles. The optimal route for any formation appears to project from a back vertex, regardless of destination. As this information is independent of the destination, it depends only on the relative weights and fixed pairs of nodes. This fairly elegant method of projecting from a back vertex can be further extended to not only solve for formations of two aircraft, but theoretically any size. As demonstrated in Refs. [29,37,44], this is done by essentially using these back vertices to create a "dummy" flight; then, all the previously described methods can be applied to create further formations between flights and dummy flights. As long as the aircraft weights, fuel-burn equations, and climb and descent distances are factored in, any number of flights can be decomposed in this way. However, the combinatorial considerations of larger formations must not be overlooked, with scalability issues arising from both the many ways of ordering of joining and breaking away from formations along with a huge increase in the number of possible formations. While much of this combinatorial complexity is due to a global, centralized approach, the use of the decentralized approach (such as that of Doole and Visser [44]) shows that scalability is possible.

A nominal rate of fuel burn for the aircraft-specific arc weightings acts only as a reasonable estimate for the final problem. Therefore, the method is adapted to move from a notion of a constant nominal fuel burn to one that changes with distance flown and weight. Furthermore, in this model, the drag-reduction benefits of flying in formation will be applied directly to the coefficient of drag via the discounting factor λ_f incorporated into the Breguet range equation [45]. The speed of each aircraft is constant for each flight section and chosen to be that which minimizes their fuel burn (or, while in formation, the total fuel burn of all members) calculated via the same range equation. As operationally flying in formation while achieving fuel savings is not always guaranteed, each aircraft is required to carry extra fuel to ensure it can fly the entire formation route solo. This is in addition to the standard requirement of a 10% fuel reserve. The takeoff weights of the aircraft are then adjusted to take this additional fuel into account. Finally, to directly compare time-free solo routes with time-free formation routes, aircraft are instructed to fly at speeds that minimize their fuel burn (or, while in formation, the total fuel burn of all members).

To summarize, the methods used in this paper are those of the geometric method for a formation with a size of two, including all these extensions outlined. These methods are used to calculate the formation routes for the results in Secs. IV–VI. By using this geometric approach for routing, it enables us to quickly calculate a cost for a potential formation. The speed of this calculation, for formations

with a size of two, allows over 100,000 possible combinations to be assessed in under 1 min.

D. Global Fleet Assignment Problem

Given that the optimized routes and costs for all possible pairings can now be easily calculated, it remains to select compatible fleets. That is, by assigning each aircraft to one formation, find the subset of all possible formations that minimizes the total cost. This is known as the *fleet assignment problem*.

Each flight can only belong to one formation (or fly solo); a mixed integer linear program (MILP) solver is used to generate the optimal subset of formations that minimizes the total cost. The optimization problem, based on similar work by Xu et al. [21], is formulated as follows: for N_a aircraft, there are N_f possible favorable formations (i.e., those with a lower cost than their respective solo flights), including N_a solo formations. A parameter of $p_{j,i} = 1$ if, and only if, aircraft i is included in formation j. Furthermore, if formation j is used, it will incur a fuel cost of c_j. The binary choice is then whether formation j is chosen in the solution (so, $x_j = 1$) or not ($x_j = 0$). Therefore, the MILP is used to optimally assign each aircraft into a formation by choosing the state of each x_j. That is,

$$\begin{aligned} \underset{x}{\text{minimize}} \quad & \sum_{j=1}^{N_f} c_j x_j, \\ \text{subject to} \quad & \sum_{j=1}^{N_f} p_{j,i} x_j = 1, \quad \forall\, i \in \{1, \ldots, N_a\}, \\ & x_j \text{ binary}, \qquad \forall\, i \in \{1, \ldots, N_a\} \end{aligned} \tag{3}$$

This MILP formulation, consisting of N_f variables and N_a constraints, can be solved using a wide range of optimization software; for this paper, we have used Gurobi [46]. The time required to solve a MILP is dependent on the number of variables and constraints; however, the solve times for the case studies presented in the following sections typically take only a few seconds.

With this in place, it is now possible to solve the following two problems: first, the routing problem to estimate the rendezvous and breakaway points for all possible formation groupings, and thus the fuel use for each; and second, the assignment problem to select a compatible set of formations from those considered to achieve minimum total fuel use for the entire fleet.

E. Aircraft Scheduling Considerations for Formation Flight

In this paper, the formation routing methods described in Sec. II optimize purely for fuel use and ignore the impact of scheduling. However, scheduling factors such as crew rosters, passenger demand, and airport capacity all influence flight timing and can be included in a multiobjective schedule optimization [21,47]. The incorporation of specific scheduling objectives in formation flight is beyond the scope of this paper. Instead, we will apply constraints on allowable change to the current schedule that the solo flights have flown. It is worth nothing that other studies [48,49] have shown that scheduling differences can often be overcome through aircraft speed changes while still producing fuel-saving formations. It has also been observed [50] that the scheduling of flights at airport hubs often operates arrivals and departures in "waves" rather that spreading them out, with an aim to minimize connection wait times of passengers and crew. This wave scheduling of many of today's flights may not be too dissimilar to those beneficial to formation flight.

Using the notation of Sec. II.D for each formation j, first, the optimal route is calculated using the methods of Sec. II; then, the aircraft speeds that minimize fuel burn (both in solo flight and in formation) are calculated. From this, the required schedule change can be measured. That is, Δt_j denotes the total change required in takeoff times, in minutes, to satisfy the formation j route. This can be accommodated via some schedule "shift" of one (or both) of the two flights by a total of Δt_j. Therefore, before solving the assignment problem of Sec. II.D, we can apply a schedule "restriction" to the N_f potential formations by filtering out any formation j that requires a Δt_j greater than some allowable schedule threshold Δ_t.

Therefore, this scheduling restriction dictates the flexibility of an aircraft to alter their takeoff time in order to potentially join other aircraft in formation. With this in mind, the results of this paper are obtained via the following three-stage solution process:

1) The first stage is enumeration: For all possible combinations, calculate the formation routes and corresponding costs.

2) The second stage is preprocess: Eliminate combinations exceeding schedule change constraint Δt.

3) The third stage is assignment: Given the costs of all combinations remaining, assign a final fleet of formations to fly in order to minimize total cost.

Note that this three-stage solution process can be extended (and has been by the authors in Refs. [29,51]) to incorporate higher-fidelity solutions. This can be done either during the first stage, which can quickly become combinatorially intractable, or after the third stage as a postprocess on the much smaller subset of assigned flights (the authors have used this approach for routing through wind only after formation assignments have been decided). Thus, at the very least, the geometric method can act as a reasonable heuristic for estimating formation potential.

III. Case Study Datasets

The focus of this paper is to look at three case studies and assess their potential for using formation flight. Given the outlined work of Sec. II, it is now possible to calculate formation routes for individual pairs of flights, cost them, and ultimately assign all aircraft into formation fleets to minimize a global cost.

A. Case Study Outline

Three case studies are chosen, each of which is defined by a list of currently operating flights: each with an origin and destination airport, an assigned aircraft type, and a current scheduled departure and arrival time.

1. *Transatlantic Airline*

The transatlantic dataset consists of 210 flights flying eastbound between the United States and Europe. Each route is based on a real flight including a specific aircraft type and scheduled departure time. These flights were taken from the OAG dataset for September 2011 [52]. While the flights have no specific company assigned to them, for the purpose of this paper, they are assumed to be in cooperation, trying to optimize savings for the entire fleet of aircraft rather than any individual airline. All 210 flights are distinct and result in 21,945 different combinations of creating formation pairs.

2. *Low-Cost Airline*

In the event of the adoption of formation flight within commercial aviation, it is possible that initially individual companies will join formations among their own fleet. As a result, this would simplify the economic problem of how to allocate and share any formation savings. The flights used are for the second largest European low-cost airline, EasyJet [53], which may have the potential to use formation flight across Europe. We refer to this flight list as the *low-cost airline* (LCA), representing a number of either short- or medium-haul flights that are typical of this kind of airline; thus, an assessment can be made for the potential for formation among shorter trips.

The dataset chosen is a typical set of flights recorded on Monday, 4 August 2014, from the FlightStats database [54]. Due to the nature of short-haul flights, many routes appeared multiple times at different times of the day, often with the same aircraft going back and forth. Thus, any formation pair combination requiring the same specific aircraft for both flights is removed by checking against the aircraft call sign and the flight number. This leaves 1313 flights, resulting in around 860,000 possible formation pair combinations, making this the largest of the three case studies.

3. Long-Haul Airline

Singapore Airlines is a major airline company serving flights from Southeast, East, and South Asia to many domestic and international destinations. It acts as a good case study for a wide range of flight distances, ranging mostly between medium-haul to super-long-haul flights. The main difference between these flights and ones seen in the other two case studies is that the vast majority of the routes are either flying from or to Singapore, like a hub-and-spoke network (discussed in Sec. III.B). The dataset contains 232 flights on the same Monday as the LCA [54], equating to just under 27,000 formation pair combinations.

B. Comparing Airline Network Design Using Graph Theory

To try to generalize the results, network characteristics will now be investigated using a graph-theoretic approach. Simple analysis of the flight network design has been depicted in Figs. 5 and 6. In these, airports are represented as nodes of a graph, whereas flights are the arcs between any two nodes. Also note that the term "degree" of a node is defined as the number of arcs incident to the node. Therefore, the degree of an airport is the total number of flights that fly to or from that airport.

With this in mind, Fig. 5 outlines the flight network as a representational graphlike structure. Then, using Fig. 5b as an example, node 1 has degree 4, whereas node 5 has degree 6. Additionally, Fig. 6 shows the sparsity of the entire network via a connectivity plot. With the airports ordered by their departure longitude on the x axis and destination longitude on the y axis, a black square is plotted at the corresponding location. With every point unique to a single flight, the more points in a column or row corresponds to a higher-degree airport.

It is observed there is a trend for domestic passenger aviation to move away from direct flights [55] to having larger airports (hubs) act as transfer points for flights, creating what is known as a hub-and-spoke network. The long-haul airline (LHA) data represent a regional airline, Singapore Airlines, which demonstrates an extreme example of a hub-and-spoke network, whereby the main hub is Singapore Changi (SIN) Airport, with the majority of their flights in some way involving SIN Airport. An example representation of this kind of network is in Fig. 5c, which resembles a "hub-and-spoke" topology with node 1 representing SIN Airport.

A hub-and-spoke network is generally distinguishable by having a single high-degree node (the hub) connected to other nodes of much lower degree. Whereas the long-haul airline flight list also has a handful of other cross connections between other airports, as a distinguishing characteristic, the majority of the flights more closely resembles this kind of hub-and-spoke arrangement. This is backed up by the network sparsity plot of Fig. 6c, showing that the entire network is focused around one node, with few flights independent of the main hub airport.

Conversely, the flights of the low-cost airline are mostly short- and medium-haul, and therefore choose to fly more point to point between many airports. This creates what more closely resembles a "connected network" (as depicted in Fig. 5b), with flights going in all directions to connect up a large geographical area (Europe in this case). However, in reality, networks like this are really just a number of hub-and-spoke networks connected together. The connectivity and sparsity of the network, shown in Fig. 6b, outlines a reasonably spread out and interconnected network, except for a hublike pattern in the center: in this case, around London Gatwick Airport.

The 210 transatlantic airline (TAA) flights are between 26 U.S. and 42 European airports, flown from west to east. As a result, the airports can be split into two disjoint sets: the U.S. departure airports and the European destination airports. In graph theory, a network of this kind is referred to as a bipartite graph (Fig. 5a). This type of flight network is not common for a single airline; rather, it is because the transatlantic airline flights are a subset of a larger set of flights. In reality, an airline company flying these transatlantic flights would likely be interconnected with many domestic flights and a range of different transcontinental flights. As can been seen from Fig. 6a, the connectivity of the flight network is very sparse. As the flights are only going in one direction (eastbound), there is none of the symmetry apparent in Fig. 6b. As they are ordered by the airports' longitudes, only the bottom right (corresponding to links between the United States and Europe) is populated.

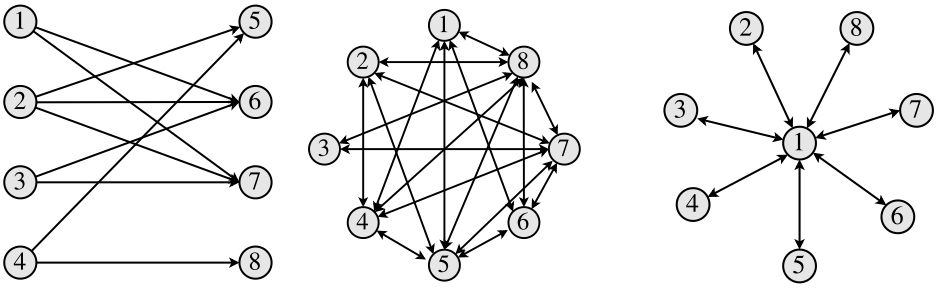

a) Bipartite network **b) Example of a more-connected network** **c) Example of a hub-and-spoke network**

Fig. 5 Representative graph structures of flight networks.

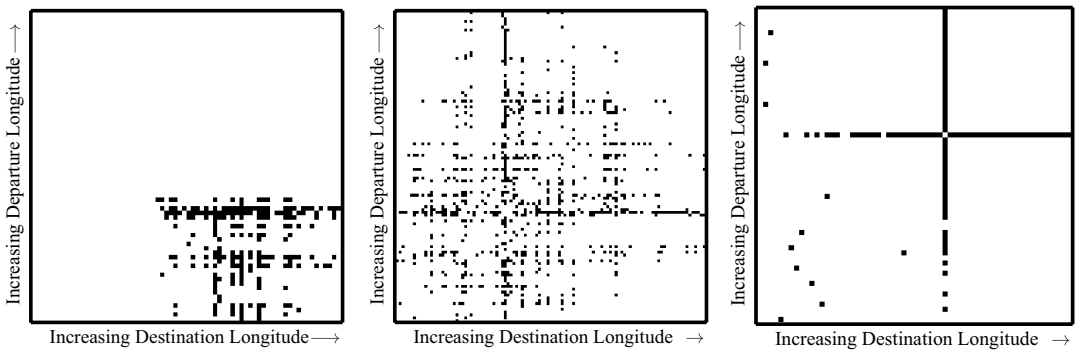

a) Transatlantic airline **b) Low-cost airline** **c) Long-haul airline**

Fig. 6 Flight network sparsity ordered by longitude.

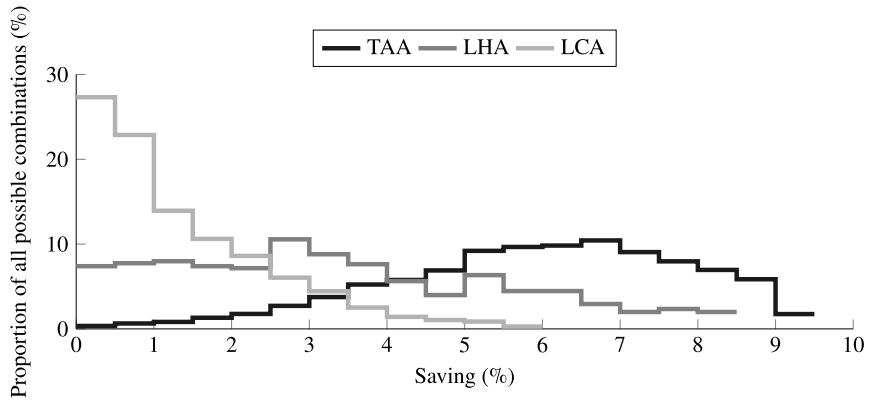

Fig. 7 Distribution of all formation combinations' formation fuel saving (in percent) for each case study.

C. Initial Results

Finally, before choosing how to assign aircraft into formations or apply scheduling restrictions, we can observe the spread of formation fuel savings (i.e., the total fuel saved between the aircraft flying in formation and flying solo) for all possible formation combinations of each case study for a formation discount factor of 10%. The "unassigned" results (i.e., all possible formation combinations found after the enumeration step of Sec. II.E) for each case study can be seen in Fig. 7. Then, all the individual formation results are counted in intervals of 0.5% fuel savings.

There is a distinct spread of formation savings for each case study, with TAA showing savings ranging all the way up to the 9–9.5% interval, with over 70% of combinations producing fuel savings over 5%. Conversely, over 50% of the formations for the LCA would produce less than 1% fuel saving and, at most, 5%. The LHA flights lie somewhere in the middle, with results spread more evenly across all of 0–8.5%. Therefore, what is clear is the three case studies selected form a reasonable representation of today's flights, as illustrated in Sec. III.B; whereas the initial results presented in Fig. 7 demonstrate distinctive ranges of potential savings.

IV. Effect of Scheduling Constraints

The following results are for creating formations with a size of two using a fixed formation discount factor of 10%, as taken from estimates in Refs. [14,15,23,28,29,37,40,41], and looking at the effect a range of flight scheduling constraints has on performance. In Sec. VI, results will also be presented for varying the discount factors. The results for each of the case studies are presented with the results shown for an increasing value of Δt (in minutes), representing the maximum total-allowable change a formation can make to their takeoff times. For lower values of Δt, there are fewer possible formations to choose from, with less choice results in lower overall savings. The focus of this section's results is to observe what happens to formation flight performance as the restrictions on the schedule are gradually lifted and the available choice of formations increases, therefore converging to the solution without schedule constraints.

A. Overall Average Formation Saving

The metric that is minimized in the MILP is the total aircraft fuel burn; therefore, the ideal measure of how good a formation assignment is, is to measure the total fuel saved between aircraft flying in formation and flying solo. For more direct comparisons, this saving, as a percentage, is shown in Fig. 8. For $\Delta t = \infty$ (i.e., the unconstrained problem, depicted as a dashed line), the overall average savings for the entire fleets are 8.89, 1.89, and 6.15% for the transatlantic airline, the low-cost airline, and the long-haul airline, respectively.

This shows a clear distinction between the three case studies, with the flights of the TAA saving the most on average and the LCA saving the least. As an entire fleet, the LCA's fuel-burn saving performance is significantly lower in comparison to the other two cases, partly due to there being many more flights, with many of them not being ideal for formation. Only around 45% of the flights in the final assignment are in formation (compared to 80–100% for the other two), thus reducing the overall averages slightly.

There are obviously very few suitable formations for a zero change in takeoff times; however, by simply allowing a Δt of just 30 min, the assignments can achieve savings reasonably close to the unconstrained problem. At around 120 min allowable change, almost all of the unconstrained formation saving is achievable for TAA and LCA. However, as shown in Figs. 8 and 9, the LHA would require greater schedule changes to achieve closer to the very maximum, with many of these involving the same long-haul routes being reused. Therefore, simply from an overall saving viewpoint, there needs to be some (but not necessarily a large amount of) flexibility in the takeoff times in order to get most of the fuel saving available from formation flight.

Our objective of minimizing fuel burn has the benefit that, by burning less fuel, airlines can proportionally spend less money on fuel; additionally, there is a proportional reduction in carbon dioxide (CO_2) emissions [56] that would have to be burned during solo flight. While fuel prices are constantly changing, a price of 600 U.S. dollars (USD) per metric tonnes (1000 kg) is the current rate as of February 2020 [57]. Additionally, the emissions index of CO_2 per kilogram of fuel burned is estimated to be roughly 3.16 [56]. Using these rates, for

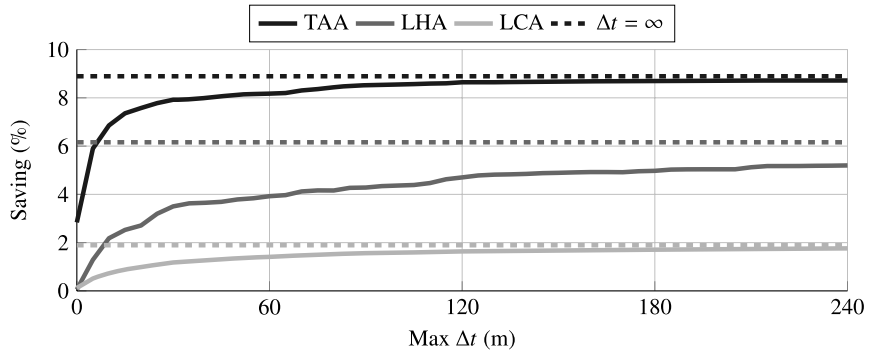

Fig. 8 Fleet average fuel savings (in percent) as a function of maximum (Max) total-allowable change in flight schedule (in minutes).

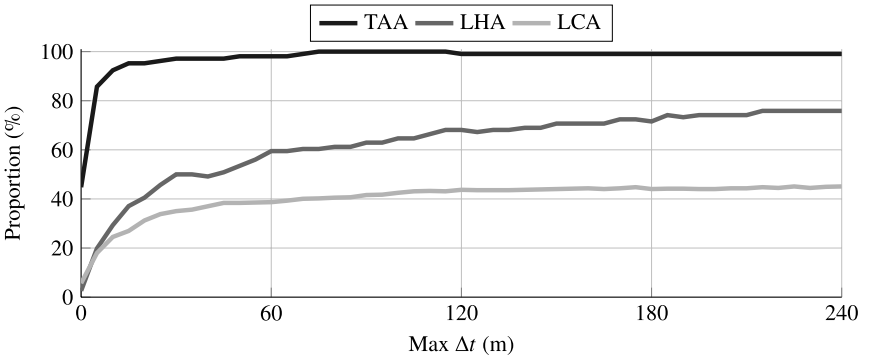

Fig. 9 Proportion of flights (in percent) assigned into formation as a function of maximum total-allowable change in flight schedule (in minutes).

scheduling restrictions of $\Delta_t = 30$ and $\Delta_t = 240$, we can see in Table 1 the huge effect reducing fuel burn has on these factors. At the top end, the 210 transatlantic flights could save over 450,000 USD each day, with around 2500 tonnes less CO_2 being emitted.

B. Proportion of Flights Joining Formation

For a given assignment, a rough guide of how well the set of flights is suited to formation flight is the proportion of formations to solo flights. The results for an increasing Δt are plotted in Fig. 9, showing the proportion of the flights that is assigned into formation instead of flying solo. For the TAA flights, there is a very rapid trend toward all flights being part of a formation (i.e., 100%). For the LHA, the approach is more gradual, eventually reaching just over 75%. The LCA has the lowest of the three but levels off fairly quickly at about 45%; however, the LCA route list is much larger than the other two at about 1300 flights. Therefore, although this overall proportion really reflects the route list as a whole, with the many hundreds of short-haul flights within the LCA flight list likely bringing down the overall percentage value, what is more important is the response to the changing Δt.

C. Flight Deviations and Common Airports

One of the fundamental drawbacks of formation flight is that aircraft may need to alter their route from their solo routes, flying out of their way in order to rendezvous with other formation members. We refer to this as the *deviation* distance (or just deviation for short), defined as the difference between the solo flight distance and the flight distance that is needed to fly in formation. Ideally, any deviation in distance flown will be compensated for by the drag-reduction formation flight offers. Intuitively, this means that formations with higher levels of deviation will be at a disadvantage because they will first need to "make up" for this offset before they can begin to make a fuel saving against flying solo.

The deviation results for the transatlantic airline, the low-cost airline, and the long-haul airline are shown in Tables 2–4, respectively. For each of these tables, the percentage of flights assigned to formation ("In formation") are values taken from the percentage curves presented in Fig. 9. The percentage of those flights in formation having a common airport (departure and/or arrival) is also detailed. The tables include the average deviation over all formations and the maximum deviation of any individual flight. These deviation results are also plotted in Figs. 10a and 10b, showing both the formation average deviation in kilometers and as a proportion of the solo distance the flights would have travelled had they not been in formation. What can be seen is that as the problem becomes less constrained; i.e., as Δt increases, the TAA flights quickly move toward lower levels of deviation. Conversely, the LCA and LHA decrease slightly, but they mostly remain fairly constant. Furthermore, it can be seen from the values outlined in Tables 2–4 that these levels of deviation are overall very low. These average deviations typically account for about 1–2% of the flight length, meaning that most flights are not going very far out of their way in order to join in formation. The maximum deviation values correspond to relatively

Table 1 Total fuel saved and the associated cost savings and reduction in CO_2

Airline	Δ_t	No. of formations	Fuel saved, tonnes	Cost, USD	CO_2, tonnes
LCA	30	230	52	31,447	166
LCA	240	296	80	47,808	252
LHA	30	58	308	184,910	974
LHA	240	88	475	285,200	1,502
TAA	30	102	769	461,389	2,430
TAA	240	104	851	510,897	2,691

Table 2 TAA: Effect of scheduling restrictions on formations

Δt, m	In formation, %	Common airport, %	Formation deviation average, km	Max, km
0	45	23	229	1125
5	86	30	183	838
10	92	29	121	691
15	95	36	112	702
30	97	47	86	485
60	98	49	76	386
120	99	51	51	352
240	99	56	40	451
∞	100	70	27	317

Table 3 LCA: Effect of scheduling restrictions on formations

Δt, m	In formation, %	Common airport, %	Formation deviation average, km	Max, km
0	6	41	52	125
5	18	36	54	239
10	25	39	47	195
15	27	43	48	195
30	35	40	47	195
60	39	42	42	239
120	44	41	36	151
240	45	44	34	143
∞	47	46	31	109

Table 4 LHA: Effect of scheduling restrictions on formations

Δt, m	In formation, %	Common airport, %	Formation deviation average, km	Max, km
0	3	100	165	281
5	20	96	135	560
10	29	97	128	560
15	37	98	123	560
30	50	98	98	515
60	59	99	113	770
120	68	99	95	1082
240	76	98	95	1289
∞	83	97	49	1140

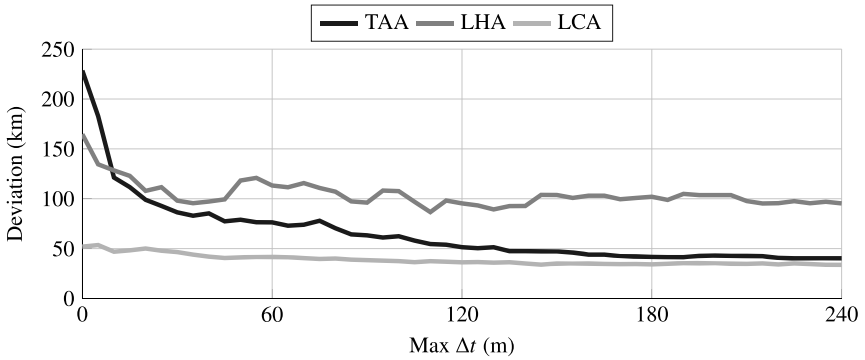

a) Formation average deviation distance (in kilometers)

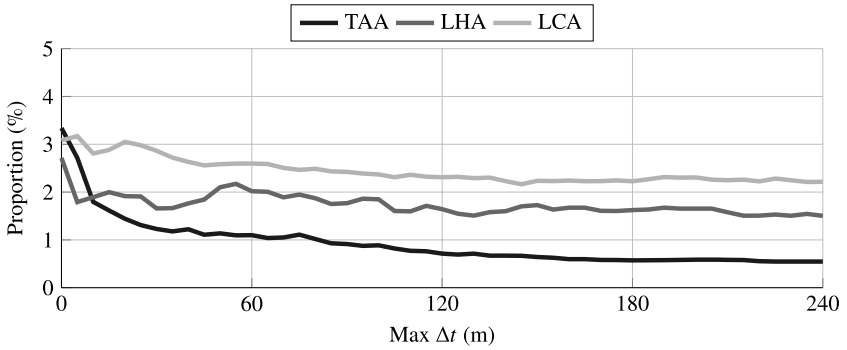

b) Formation average deviation as a proportion (%) of solo distance

Fig. 10 Deviation required for formation flight as a function of maximum total-allowable change in flight schedule (in minutes).

few formations, and thus the results tend to be spread. It is therefore worth noting that even with low average savings, there may still be a few formations that have to deviate a larger amount. Importantly, these relatively small increases to route distances mean that total flight times would not be hugely effected. The average deviation range between 27 and 229 km at an example cruise speed of 825 km/h equates to between 2 and 17 min, respectively.

A linked factor to the level of deviation is whether the flights making up a formation have a common airport: that is, if they either depart from or arrive at the same airport as the other formation member. Clearly, if an airport is shared, then there is likely to be a lower level of deviation. It is worth recalling from Sec. II.C that we take into account climb and descent sections of the flight where formation saving is not allowed; thus, sharing an airport simply removes the deviation required for the rendezvous and/or breakaway portion of the flight. The proportions of the assigned formations who share a common airport are in Tables 2–4, with values plotted in Fig. 11. Due to the type of network explored in Sec. III.B, the LHA flights almost all fly to or from Singapore Changi Airport. The LCA flights are also more or less constant at a level of about 40%, whereas the TAA flights trend toward about 55%. However, while increases in Δt show little impact on the levels of deviation of Fig. 10 or the shared airports of Fig. 11 for the LHA and the LCA flights, the transatlantic flights' trend toward lower deviation is matched by an increase in proportion of common airports.

V. Suitability of Formation Flight

The results of Sec. IV clearly demonstrate the potential for commercial formation flight to achieve significant fuel savings even with scheduling constraints. However, it is important to be able to assess, at the macrolevel, how well a particular set of flights, airlines, or geographical regions are suited to the use of formation flight. In Sec. V.A, we will outline a single metric of *utilization*, which is capable of quantifying this idea suitably and enables us to easily compare distinct case studies. Additionally, being able to demonstrate any possible *predictive indicators* for what is more likely to result in good formation savings is key to understanding potential. Therefore, in Sec. V.B, we look at correlations between single flight and formation characteristics that equate to the best savings.

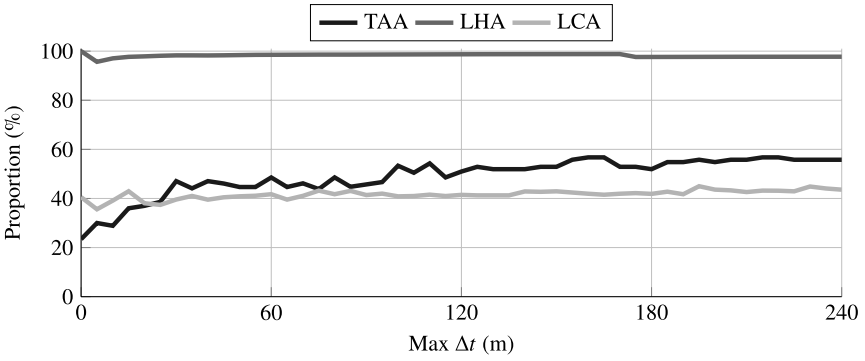

Fig. 11 Proportion of formations that share a common airport as a function of maximum total-allowable change in flight schedule (in minutes).

A. Utilization

To make more suitable comparisons between distinct case studies, we must assess how well an assignment performs when compared to the maximum-achievable potential of the routes. If a formation pair has a formation discount factor of 10%, this means that if both aircraft started and finished in formation, observing the fuel-burn saving over the entire flight, the maximum-achievable saving would be 10%. However, as aircraft obviously need time to climb and descend, and so cannot save fuel over the entire flight, the actual maximum-achievable saving will vary per flight. The notion of the utilization, denoted as k, is the proportion of saving achieved to the maximum achievable. That is, the utilization factor k measures much of the potential fuel-saving is lost due to increases in deviation and cruise distance in order to reach rendezvous and separation points. To quantify this, first the great circle distance of the solo flight is taken; as noted in Sec. II.C, we only consider the cruise portion of flight, and so the distance required to climb and descend is deducted. Then, the differential fuel-burn model is applied to the remaining (cruise) distance to calculate the solo fuel burn (SFB). The formation fuel burn (FFB) for this ideal solo cruise distance, for a given formation discount factor, is also calculated; and the difference between this and the solo fuel burn represents the maximum-achievable saving (MAS) $=$ SFB $-$ FFB. The utilization k is the percentage of achieved saving (AS) to the maximum-achievable saving (MAS), $k = (\mathrm{AS}/\mathrm{MAS})$. For example, saving 8% when there is a maximum possible of 9% (as climb/descent has been taken into account) results in a utilization of roughly 89%. To use this metric for a set of flights, the utilization k is simply the sum of all AS_s divided by the sum of all MAS_s as a percentage. With this, the utilization metric can be used to quickly express how well suited a group of flights is to flying in formation.

The values are plotted in Fig. 12 and show a clear distinction between the three case studies. The TAA flights can achieve anywhere up to a very impressive 96% utilization for $\Delta t = \infty$; that is, out of the 9.3% theoretical-maximum savings achievable, roughly 8.9% was realized. The LCA and LHA flights, respectively, can achieve levels of utilization of up to roughly 35 and 75%.

The utilization factor is a result of a number of different components, such as geographical suitability and flight distance, but importantly dictated by the theoretical maximum. As aircraft are only considered to be in formations during the cruise leg of their flights, this theoretical maximum is calculated based on each flight being in formation for the entire cruise proportion of its flight. Therefore, a higher proportion of cruise to noncruise flights equates to a greater theoretical-maximum saving. For the TAA, LCA, and LHA, these proportion are 9.3, 5.2, and 8.2%, respectively, and remain constant for all Δt because they are based on the solo flight list, and therefore do not change based on assignment.

These results show that as the scheduling constraint is gradually lifted, values tend toward their unconstrained ideal. It is clear from Sec. IV.A that even with a relatively low Δt of 30 min., formations can still achieve very reasonable savings. While Sec. IV.C shows a general tendency to move toward lower levels of deviation (with transatlantic flights being the most affected), this corresponds to more formations sharing a common airport. Finally, the utilization factors of Sec. V.A show that the TAA flights are the best suited to formation, followed by the LHA and then by the LCA flights, with the proportion of cruise to noncruise flights being a major contributor.

B. Flight Characteristic Correlations

The results of Sec. IV look at summarizing values for a collection of results, i.e., averages, maximums, and minimums for an assignment of formations. To try to understand and predict the results, and in turn identify factors that affect formation flight performance, we look at correlations. With the correlation coefficient of two variables X and Y, $\rho_{X,Y}$ is between $+1$ and -1 inclusive, with 0 meaning no correlation, 1 meaning a perfect positive correlation, and -1 total negative correlation. The stronger a correlation (i.e., the higher the absolute value), the stronger the dependence between the two variables. A strong positive correlation means that an increase in X will likely result in an increase in Y, whereas a strong negative correlation would mean an increase in X would likely result in a decrease in Y.

For the optimal assignments, based on a Δt of 30 min, for the TAA, LCA, and LHA, some results are plotted in Figs. 13–15. Each point

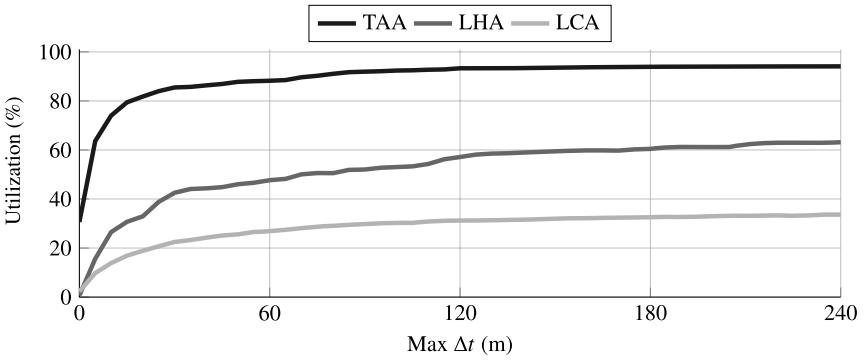

Fig. 12 Utilization of potential formation saving as a function of maximum total-allowable change in flight schedule (in minutes).

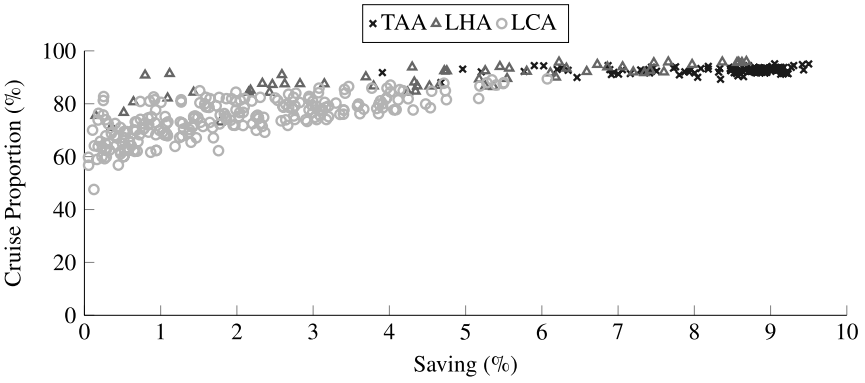

Fig. 13 Cruise proportion against saving. MILP assignment for $\Delta t = 30$. Correlation: TAA $= 0.67$, LCA $= 0.74$, and LHA $= 0.82$.

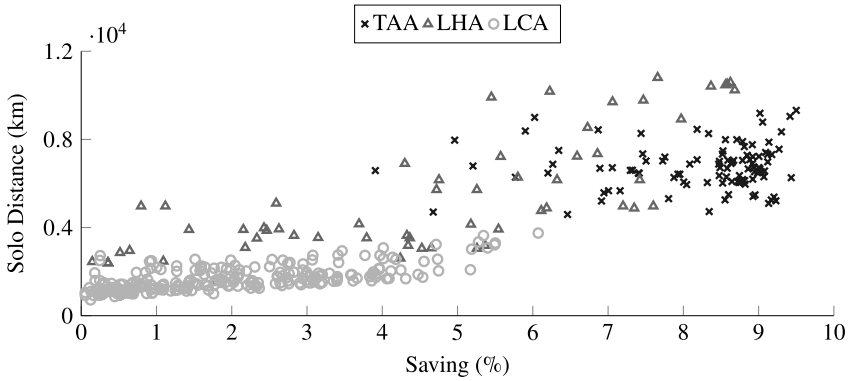

Fig. 14 Solo distance against saving. MILP assignment for $\Delta t = 30$. Correlation: TAA = 0.07, LCA = 0.70, and LHA = 0.70.

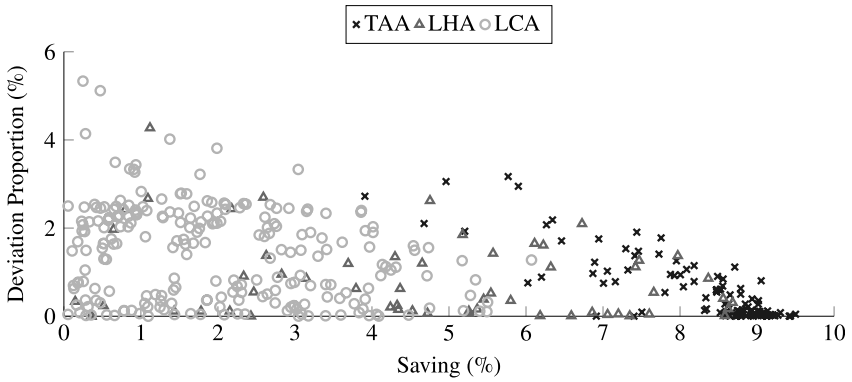

Fig. 15 Deviation proportion against saving. MILP assignment for $\Delta t = 30$. Correlation: TAA = −0.79, LCA = 0.01, and LHA = −0.16.

on these graphs corresponds to an assigned formation, with the location representing the relationship between the saving percentage and some other chosen variable; importantly, the level of correlation is also noted.

Looking solely at the x locations (i.e., the formation saving), one sees the same pattern that is observable in Fig. 7. That is, the trans-atlantic flights are negatively skewed toward the higher-percentage saving, the low-cost airline skews positively toward the lower savings, and the long-haul airline flights spread more evenly across the entire range. The results of this section aim to explore the main impacting factors on these formation savings.

Observing the relationship between cruise proportion (discussed in Sec. V.A) and saving, the plot in Fig. 13 clearly shows a positive trend toward higher savings through a higher proportion of cruise flight; whereas for the higher levels of saving, proportions of 80–90% are required, and there are formations with that level of cruise proportion achieving much lower savings. This trend is backed up by a strong positive correlation between saving and cruise proportion, with TAA = 0.67, LCA = 0.74, and LHA = 0.82.

Additionally, Fig. 14 shows the percentage of savings against the solo formation distance. While solo distance is essentially a fixed input rather than a result, it is an aspect that has direct effect on the cruise proportion and deviation. This spread of results shows a general trend toward higher saving along with a higher solo distance; whereas the LCA and LHA have a strong positive correlation, there is almost no correlation for the TAA flights. Notably, what it really shows is that there is more of a barrier to higher-percentage savings. Formations likely need to be longer than 4000 km to achieve savings over 6%, which in turn would mean a cruise proportion likely above 80%. Conversely, longer flights do not guarantee higher savings percentages because there are many flights achieving 6–7%, which are substantially longer than those with 9%.

Finally, the relationship between the proportion of deviation to solo distance and the saving percentage is plotted in Fig. 15. While the spreads show formations with a high proportion of deviation likely result in lower savings, this is most apparent for the TAA flights, which have a strong negative correlation of −0.79. Additionally, when comparing the unassigned formations to those which are assigned for a Δt of 30 min, there is minimal change. The same conclusions about the correlations can be made for both the assigned and the unassigned results. At most, the changes are around 0.2 in either direction, mainly shifting those from minimally correlated to totally uncorrelated, and vice versa. Importantly, what this implies is that these correlations are mostly a feature of the case study and not the assignment process.

The correlation between saving and deviation differs between case studies. Deviation, which has a strong negative correlation for the TAA flights (−0.79), has almost no correlation for the LCA (0.01) and LHA (−0.16) flights. As can be seen in Fig. 10 and Tables 2–4, the LCA and LHA flights have a much higher level of deviation present than the TAA. Thus, as most flights have a reasonable amount of deviation, this becomes less of a differentiating feature between formations.

Therefore, if given a more diverse range of flights lists such as the LCA and LHA flights, the indicators of formations with potentially high-percentage savings are different from that of the TAA flights. One should aim for flights that have a longer solo distance because they will be able to offset deviations and achieve higher cruise proportions, and thus more savings.

VI. Sensitivity to Formation Discount

Throughout this paper, for formations with a size of two, a fuel-saving discount of 10% has been assumed when flying in formation. However, due to this value only being an estimate, based on a variety of aerodynamic models and flight tests [14,15,23,28,40,41], it is important to observe what effect this value has on the overall saving.

Therefore, we now look at the routing and assignment results for the three flight case studies for the problem with no scheduled constraints (i.e., $\Delta t = \infty$). The results for an increasing formation discount factor, as a percentage, between 1 and 20%, are now presented. For clarification, let us first define the formation discount $\hat{\lambda}_f$ as the percentage of fuel saving applied during the formation stage of flight. This value

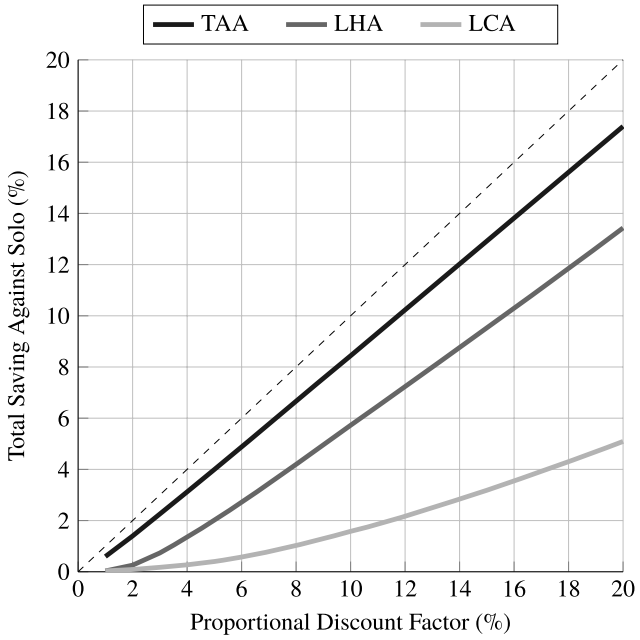

Fig. 16 Relation between discount factor and overall saving achieved.

relates to the value λ_f of Sec. II by $\hat{\lambda}_f = 100 \times (1 - \lambda_f)$, and it is essentially the same value expressed as a percentage.

Lower values of $\hat{\lambda}_f$ mean a lower level of incentive for flying in formation, whereas higher levels increase this incentive. The focus of this section is to observe the effect on the measures introduced in Sec. IV as the incentive for flying in formation is increased or decreased.

A. Overall Average Formation Saving

The overall objective is to minimize cost, which is analogous to maximizing saving; therefore, all flights are aiming for the best percentage saving they can achieve. The overall saving as a percentage of solo flight is shown in Fig. 16. A range of possible savings is present in the results for differing $\hat{\lambda}_f$, with the same general ordering of the TAA doing "best," followed by the LHA and the LCA. What is important to observe in these results is the shape of the curve and the response to an increase/decrease in $\hat{\lambda}_f$. The results for the transatlantic show a stronger linear relationship between $\hat{\lambda}_f$ and overall saving, whereas the other two have more of an offset with less direct response.

B. Proportion of Flights Joining Formation

The suitability of a list of flights for formation flight can be shown by the proportion of formations to solo flights. The results of Fig. 17 show that the TAA flights are highly suited to formation flight, even for very low discount factors. While the LHA grows to around 80%, the proportion begins very low and shows a level of unsuitability for $\hat{\lambda}_f$ less than about 5%. Finally, the growth for the LCA flights is very steady (almost linear) between 1 and 20%, but for much lower proportions, with many unsuited to formation flight.

C. Flight Deviations

The deviation results for the TAA, LCA, and LHA are plotted in Figs. 18a and 18b, showing both the formation average deviation in kilometers and as a proportion of the solo distance. What can be seen is that while deviation should be incentivized by greater levels of $\hat{\lambda}_f$, the levels of deviation do not change by much. Similarly, for low formation discounts, the "return" of flying in formation gets proportionally more offset by the deviation involved. The results shown for the LCA in Fig. 18b support this, where low $\hat{\lambda}_f$ means only small deviations are economical; but, as the discount factor increases, so too does the "freedom" to change course and fly in formation as greater savings are available.

Strongly linked to the level of deviation is the proportion of flights with a common airport. The proportion of the assigned formations who share a common airport is plotted in Fig. 19. Whereas the LHA flights almost all fly to or from Singapore Changi Airport, the LCA and TAA flights move toward a greater proportion of shared airports as $\hat{\lambda}_f$ increases. As a result, with the number of shared airports increasing and the level of deviation generally remaining more constant, the deviations must therefore be shifted to the joining or the breaking section of the flight. That is, formations taking off from the same airport likely have destinations that are further apart (and vice versa).

D. Utilization

As outlined in Sec. V.A, the level of utilization depicts the efficiency of the overall formation process. The results plotted in Fig. 20, between the three case studies, show a general tendency toward higher utilization for higher levels of $\hat{\lambda}_f$. The TAA flights quickly achieve high utilization levels. The LHAs require a $\hat{\lambda}_f$ of roughly 18% before they reach a level of 80% utilization, whereas the LCA flights more gradually approach more modest levels of up to 50% for a $\hat{\lambda}_f$ of 20%.

The results of this section have explored the effect the formation discount factor $\hat{\lambda}_f$ has on the characteristics of formation flight. While the value for $\hat{\lambda}_f$ has been estimated anywhere between 1 and 20% in the literature, these results clearly demonstrate the direct effect this value has on the potential formation savings and the assigned formation flight choices. Although it is clear that greater discount factors should result in higher overall savings, this effect is not the same for all sets of flights. Notably, in the cases of both the TAA and LHA, the relationship between drag reduction and fuel saving at a fleet level is almost directly proportional, along with the measures of utilization show that these flights are the most efficient at converting drag reduction into achievable fuel savings.

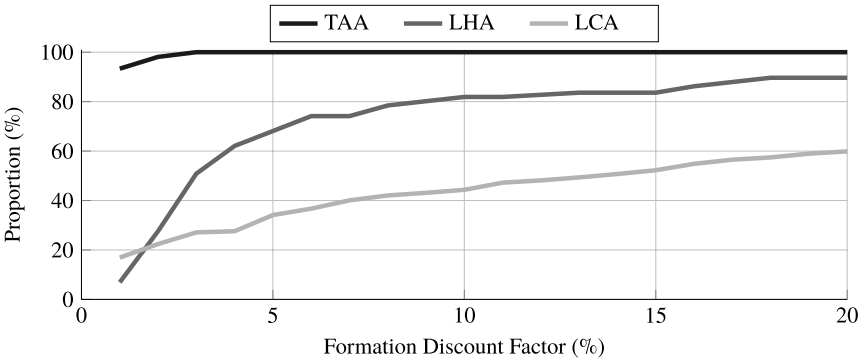

Fig. 17 Proportion of aircraft assigned into a formation as a function of formation discount factor.

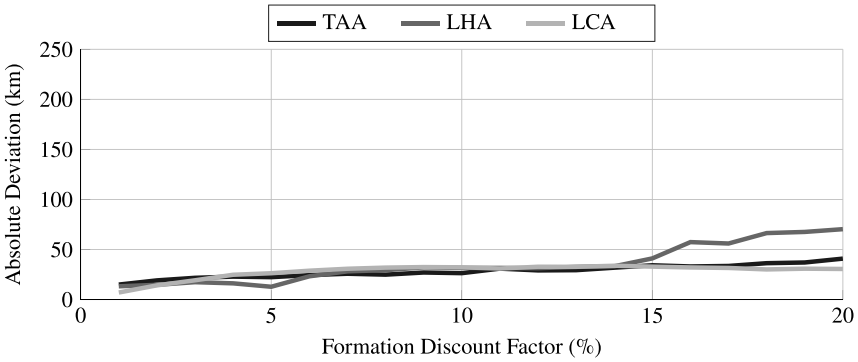

a) Formation average deviation distance

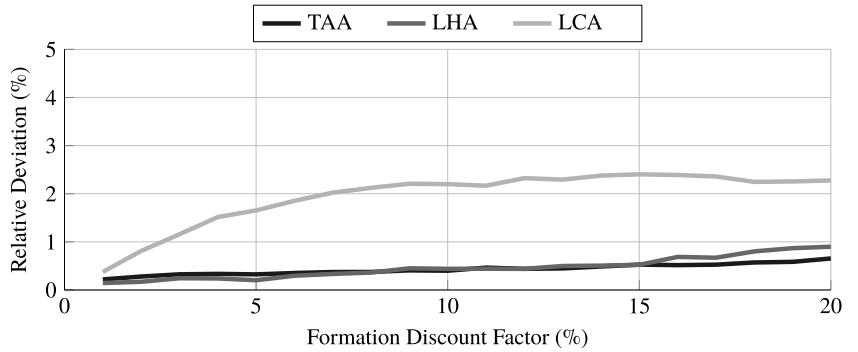

b) Formation average deviation as a proportion of both flight

Fig. 18 Deviation in distance between solo and formation flight as a function of formation discount factor.

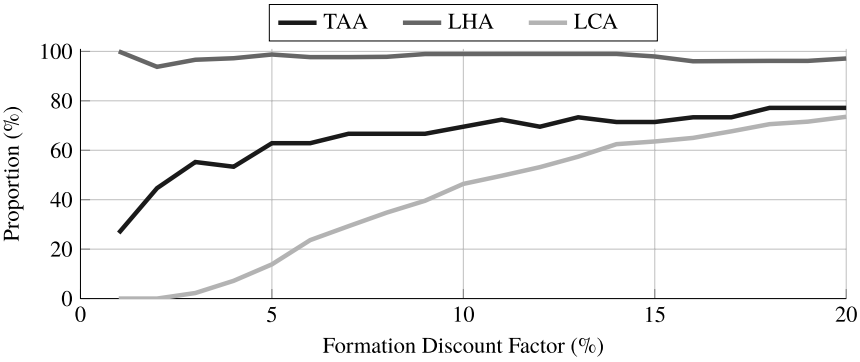

Fig. 19 Proportion of formations that share a common airport.

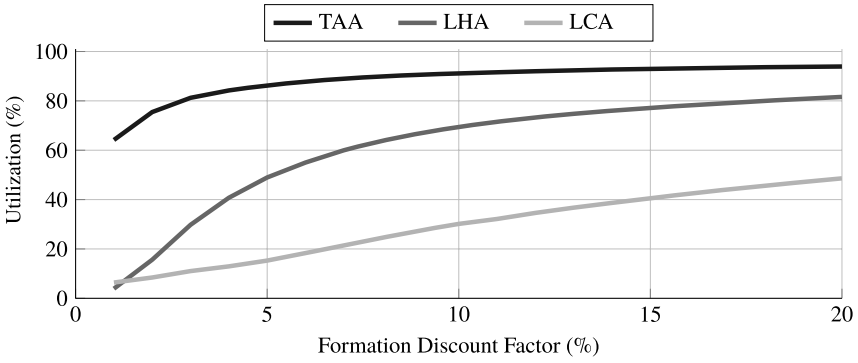

Fig. 20 Utilization (in percent) as a function of formation discount factor.

VII. Conclusions

This paper has explored the potential formation flight savings of three distinct case studies consisting of a list of solo flights. The transatlantic airline routes consisted entirely of long-haul flights flying east from the United States to Europe: the low-cost airline routes were based in Europe and either short or medium haul, whereas the long-haul airline routes ranged from medium- to super-long-haul flights, all across Southeast Asia.

The results of running the routing and assignment of all formation combinations for each case study were explored for a formation discount factor $\hat{\lambda}_f$ of 10%. The overall average percentage fuel savings were promising for all the flight lists, with the transatlantic airline performing best at close to 9%, followed by the long-haul airline at just over 6%, whereas the low-cost airline flights produced a savings of just under 2%, showing that there is real potential even for the short-haul flights. By exploring the impact scheduling restrictions would have on the number of potential flight formations, it was shown that with an allowable change in takeoff time, in as little as little as 30 min, very reasonable fuel savings can be had across the fleet.

Introduced in this paper is a general measure of suitability, called utilization, which gives an indication of those flight lists that are better suited for formation flight. Particularly high levels (95%) of utilization were shown for the TAA routes; slightly less was shown (75%) for the LHA; and reasonably low levels (35%) were shown for the LCA flights.

An analysis of the correlation between key variables showed what features of a set of flights are indicative of producing good formations for overall fleet fuel savings. Low levels of deviation were important for TAA flights, generally resulting in better savings. Conversely for the LCA and LHA flights, the longer solo flight distances provided greater fuel-saving potential than the shorter flights. Thus, we can conclude that the predictors of formation potential are mostly related to maximum time in cruise flight and minimal deviation to join other formation members. Interestingly, it was shown that the scheduling constraint was entirely uncorrelated to formation saving, acting more or less like a random filter, removing potential choices within the assignment stage.

The results for a range of possible formation discount factors between 1 and 20% showed that the relationship between fuel saving and different values of $\hat{\lambda}_f$ was almost directly proportional. Notably, in the cases of both the TAA and LHA, the relationship between drag reduction and fuel saving was almost linear, along with the measures of utilization showing that these flights are the most efficient at converting drag reduction into achievable fuel savings. Furthermore, even though greater deviation was incentivized at higher rates of drag reduction $\hat{\lambda}_f$, this did not result in a large increase in average deviations. Instead, formation routes shifted toward sharing airports and leaving all flight deviations to one end of the formation route.

The methods and results presented in this paper help to highlight the boundaries of the trade space for routing and assignment when considering the use of formation flight in the commercial world. Important, it also demonstrates a level of robustness to airline and flight types not explored anywhere else. The results shown are indicative of potential but also open up several interesting avenues for future work. The methods presented can be used to calculate larger formations; therefore, a much more in-depth analysis of the potential and limitations of big formation fleets is a natural extension that should be explored. Additionally, while scheduling has been discussed, the authors believe a more holistic investigation of the factors contributing to an airline's direct operating costs, such as scheduling as well as flight time and delay implications, would be of significant interest to the research community.

Acknowledgments

The authors wish to thank the Engineering and Physical Sciences Research Council for the ongoing support of this research. The authors are also grateful to Hendrikus Visser, Ilan Kroo, and Andrew Ning for interesting and motivating discussions on this topic.

References

[1] Poli, R., Ravenel, L., and Besson, R., "The International Air Transport Association (IATA) Annual Review 2018," *74th Annual General Meeting Sydney*, June 2018.

[2] Suh, D. Y., and Ryerson, M. S., "Forecast to Grow: Aviation Demand Forecasting in an Era of Demand Uncertainty and Optimism Bias," *Transportation Research, Part E*, Vol. 128, July 2019, pp. 400–416. https://doi.org/10.1016/j.tre.2019.06.016

[3] Forsyth, P., "The Impacts of Emerging Aviation Trends on Airport Infrastructure," *Journal of Air Transport Management*, Vol. 13, No. 1, 2007, pp. 45–52. https://doi.org/10.1016/j.jairtraman.2006.10.004

[4] Dareck, M., Edelstenn, C., and Ender, T., "Flightpath 2050 Europe's Vision for Aviation," European Commission TR KI-31-11-098-EN-C, 2011. https://doi.org/10.2777/50266

[5] Antoine, N. E., and Kroo, I. M., "Aircraft Optimization for Minimal Environmental Impact," *Journal of Aircraft*, Vol. 41, No. 4, 2004, pp. 790–797. https://doi.org/10.2514/1.71

[6] Edwards, H. A., Dixon-Hardy, D., and Wadud, Z., "Aircraft Cost Index and the Future of Carbon Emissions from Air Travel," *Applied Energy*, Vol. 164, Feb. 2016, pp. 553–562. https://doi.org/10.1016/j.apenergy.2015.11.058

[7] Dray, L., "An Analysis of the Impact of Aircraft Lifecycles on Aviation Emissions Mitigation Policies," *Journal of Air Transport Management*, Vol. 28, May 2013, pp. 62–69. https://doi.org/10.1016/j.jairtraman.2012.12.012

[8] Nangia, R. K., "'Greener' Civil Aviation Using Air-to-Air Refuelling–Relating Aircraft Design Efficiency and Tanker Offload Efficiency," *Aeronautical Journal*, Vol. 111, No. 1123, 2007, pp. 589–592. https://doi.org/10.1017/S0001924000001858

[9] Qin, N., Vavalle, A., Le Moigne, A., Laban, M., Hackett, K., and Weinerfetl, P., "Aerodynamic Considerations of Blended Wing Body Aircraft," *Progress in Aerospace Sciences*, Vol. 40, No. 6, 2004, pp. 321–343. https://doi.org/10.1016/j.paerosci.2004.08.001

[10] Bower, G., Flanzer, T. C., and Kroo, I., "Formation Geometries and Route Optimization for Commercial Formation Flight," *27th AIAA Applied Aerodynamics Conference*, AIAA Paper 2009-3615, 2009. https://doi.org/10.2514/6.2009-3615

[11] Haissig, C., "Military Formation Flight as a Model for Increased Capacity in Civilian Airspace," *23rd Digital Avionics Systems Conference*, Inst. of Electrical and Electronics Engineers, New York, 2004, pp. 1.C.4–1.1–9. https://doi.org/10.1109/DASC.2004.1391244

[12] DeVries, L., and Paley, D. A., "Wake Estimation and Optimal Control for Autonomous Aircraft in Formation Flight," *AIAA Guidance, Navigation, and Control (GNC) Conference*, AIAA Paper 2013-4705, 2013. https://doi.org/10.2514/6.2013-4705

[13] Ning, S. A., Flanzer, T. C., and Kroo, I., "Aerodynamic Performance of Extended Formation Flight," *Journal of Aircraft*, Vol. 48, No. 3, 2011, pp. 855–865. https://doi.org/10.2514/1.C031046

[14] Blake, W., and Multhopp, D., "Design, Performance and Modeling Considerations for Close Formation Flight," *23rd Atmospheric Flight Mechanics Conference*, AIAA Paper 1998-4343, 1998. https://doi.org/10.2514/6.1998-4343

[15] Blake, W., and Gingras, D. R., "Comparison of Predicted and Measured Formation Flight Interference Effects," *Journal of Aircraft*, Vol. 41, No. 2, 2004, pp. 201–207. https://doi.org/10.2514/1.9278

[16] Jacques, D., Pachter, M., Wagner, G., and Blake, B., "An Analytical Study of Drag Reduction in Tight Formation Flight," *AIAA Atmospheric Flight Mechanics Conference and Exhibit*, AIAA Paper 2001-4075, 2001. https://doi.org/10.2514/6.2001-4075

[17] Wagner, M. G., Jacques, L. D., Blake, W., and Pachter, M., "Flight Test Results of Close Formation Flight for Fuel Savings," *AIAA Atmospheric Flight Mechanics Conference*, AIAA Paper 2002-4490, 2002. https://doi.org/10.2514/6.2002-4490

[18] Vachon, M. J., Ray, R., Walsh, K., and Ennix, K., "F/A-18 Aircraft Performance Benefits Measured During the Autonomous Formation Flight Project," *AIAA Atmospheric Flight Mechanics Conference*, AIAA Paper 2002-4491, 2002. https://doi.org/10.2514/6.2002-4491

[19] Ray, R., Cobleigh, B., Vachon, M. J., and St. John, C., "Flight Test Techniques Used to Evaluate Performance Benefits During Formation Flight," *AIAA Atmospheric Flight Mechanics Conference*, AIAA Paper 2002-4492, 2002. https://doi.org/10.2514/6.2002-4492

[20] Xu, J., Ning, S., Bower, G., and Kroo, I., "Aircraft Route Optimization for Heterogeneous Formation Flight," *53rd AIAA/ASME/ASCE/AHS/ASC Structures, Structural Dynamics and Materials Conference*, AIAA Paper 2012-1524, 2012. https://doi.org/10.2514/6.2012-1524

[21] Xu, J., Andrew Ning, S., Bower, G., and Kroo, I., "Aircraft Route Optimization for Formation Flight," *Journal of Aircraft*, Vol. 51, No. 2, 2014, pp. 490–501. https://doi.org/10.2514/1.C032154

[22] Unterstrasser, S., and Stephan, A., "Far Field Wake Vortex Evolution of Two Aircraft Formation Flight and Implications on Young Contrails," *Aeronautical Journal*, Vol. 124, No. 1275, 2020. https://doi.org/10.1017/aer.2020.3

[23] Liu, Y., and Stumpf, E., "Estimation of Vehicle-Level Fuel Burn Benefits of Aircraft Formation Flight," *Journal of Aircraft*, Vol. 55, No. 2, 2017, pp. 1–9. https://doi.org/10.2514/1.C034296

[24] Voskuijl, M., "Cruise Range in Formation Flight," *Journal of Aircraft*, Vol. 54, No. 6, 2017, pp. 2184–2191. https://doi.org/10.2514/1.C034246

[25] Brodecki, M., and Subbarao, K., "Autonomous Formation Flight Control System Using In-Flight Sweet-Spot Estimation," *Journal of Guidance, Control, and Dynamics*, Vol. 38, No. 6, 2015, pp. 1083–1096. https://doi.org/10.2514/1.G000220

[26] Zhang, Q., and Liu, H. H., "Aerodynamics Modeling and Analysis of Close Formation Flight," *Journal of Aircraft*, Vol. 54, No. 6, 2017, pp. 2192–2204. https://doi.org/10.2514/1.C034271

[27] DeVries, L., and Paley, D. A., "Wake Sensing and Estimation for Control of Autonomous Aircraft in Formation Flight," *Journal of Guidance, Control, and Dynamics*, Vol. 39, No. 1, 2016, pp. 32–41. https://doi.org/10.2514/1.G001138

[28] Blake, W. B., and Flanzer, T. C., "Optimal Routing for Drag-Reducing Formation Flight: A Restricted Case," *Journal of Guidance, Control, and Dynamics*, Vol. 39, No. 1, 2016, pp. 173–176. https://doi.org/10.2514/1.G001350

[29] Kent, T. E., and Richards, A. G., "Analytic Approach to Optimal Routing for Commercial Formation Flight," *Journal of Guidance, Control, and Dynamics*, Vol. 38, No. 10, 2015, pp. 1872–1884. https://doi.org/10.2514/1.G000806

[30] Verhagen, C. M., Visser, H. G., and Santos, B. F., "A Decentralized Approach to Formation Flight Routing of Long-Haul Commercial Flights," *Journal of Aerospace Engineering*, Vol. 233, No. 8, 2019, pp. 2992–3004. https://doi.org/10.1177/0954410018791068

[31] Ribichini, G., and Frazzoli, E., "Efficient Coordination of Multiple-Aircraft Systems," *42nd IEEE International Conference on Decision and Control (IEEE Cat. No. 03CH37475)*, Vol. 1, Inst. of Electrical and Electronics Engineers, New York, 2003, pp. 1035–1040. https://doi.org/10.1109/CDC.2003.1272704

[32] Ning, S. A., Kroo, I., Aftosmis, M. J., Nemec, M., and Kless, J. E., "Extended Formation Flight at Transonic Speeds," *Journal of Aircraft*, Vol. 51, No. 5, 2014, pp. 1501–1510. https://doi.org/10.2514/1.C032385

[33] Mason, W., and Iglesias, S., "Optimum Spanloads in Formation Flight," *40th AIAA Aerospace Sciences Meeting and Exhibit*, AIAA Paper 2002-0258, 2002. https://doi.org/10.2514/6.2002-258

[34] Okolo, W., Dogan, A., and Blake, W., "Effect of Trail Aircraft Trim on Optimum Location in Formation Flight," *Journal of Aircraft*, Vol. 52, No. 4, 2015, pp. 1201–1213. https://doi.org/10.2514/1.C032865

[35] Pachter, M., D'Azzo, J. J., and Proud, A. W., "Tight Formation Flight Control," *Journal of Guidance, Control, and Dynamics*, Vol. 24, No. 2, 2001, pp. 246–254. https://doi.org/10.2514/2.4735

[36] Weihua, Z., and Go, T. H., "Robust Decentralized Formation Flight Control," *International Journal of Aerospace Engineering*, Vol. 2011, Sept. 2011, pp. 1–13. https://doi.org/10.1155/2011/157590

[37] Kent, T. E., "Optimal Routing and Assignment for Commercial Formation Flight," Ph.D. Thesis, Univ. of Bristol, Bristol, England, U.K., 2015. https://doi.org/10.13140/RG.2.2.27277.74721

[38] Nuic, A., "User Manual for the Base of Aircraft Data (BADA) Revision 3.6," EUROCONTROL Experimental Center, Bretigny, France, 2005, pp. 1–87, https://www.eurocontrol.int/sites/default/files/library/022_BADA_User_Manual.pdf [accessed 7 Sept. 2014].

[39] Kent, T. E., and Richards, A. G., "A Geometric Approach to Optimal Routing for Commercial Formation Flight," *AIAA Guidance, Navigation, and Control (GNC) Conference*, AIAA Paper 2012-4769, 2012. https://doi.org/10.2514/6.2012-4769

[40] King, R., and Gopalarathnam, A., "Ideal Aerodynamics of Ground Effect and Formation Flight," *Journal of Aircraft*, Vol. 42, No. 5, 2005, pp. 1188–1199. https://doi.org/10.2514/1.10942

[41] Lissaman, P. B. S., and Shollenberger, C. A., "Formation Flight of Birds," *Science*, Vol. 168, No. 3934, 1970, pp. 1003–1005. https://doi.org/10.1126/science.168.3934.1003

[42] Gueron, S., and Tessler, R., "The Fermat-Steiner Problem," *American Mathematical Monthly*, Vol. 109, No. 5, 2002, pp. 443–451. https://doi.org/10.1080/00029890.2002.11919871

[43] de Villiers, M. D., "A Generalisation of the Fermat-Torricelli Point," *Mathematical Gazette*, Vol. 79, No. 485, 1995, pp. 374–378. https://doi.org/10.2307/3618319

[44] Doole, M., and Visser, H. G., "A Multi-Stage Centralized Approach to Formation Flight Routing and Assignment of Long-Haul Airline Operations," *Proceedings of the 4th International Conference on Vehicle Technology and Intelligent Transport Systems*, Vol. 1, SciTePress, 2018, pp. 47–58. https://doi.org/10.5220/0006661800470058

[45] Anderson, J. D., *Introduction to Flight*, 3rd ed., McGraw–Hill Series in Aeronautical and Aerospace Engineering, McGraw–Hill, New York, 2000, pp. 310–322.

[46] Gurobi Optimization, LLC, "Gurobi Optimizer Reference Manual," 2019, https://www.gurobi.com/documentation/8.1/refman/index.html [retrieved 30 Sept. 2019].

[47] Bayen, A., and Tomlin, C., "MILP Formulation and Polynomial Time Algorithm for an Aircraft Scheduling Problem," *42nd IEEE International Conference on Decision and Control (IEEE Cat. No. 03CH37475)*, Inst. of Electrical and Electronics Engineers, New York, 2003, pp. 5003–5010. https://doi.org/10.1109/CDC.2003.1272423

[48] Hartjes, S., van Hellenberg Hubar, M. E., and Visser, H. G., "Multiple-Phase Trajectory Optimization for Formation Flight in Civil Aviation," *CEAS Aeronautical Journal*, Vol. 10, No. 2, 2019, pp. 453–462. https://doi.org/10.1007/s13272-018-0329-9

[49] Kent, T. E., and Richards, A. G., "Accounting for the Effect of Ground Delay on Commercial Formation Flight," *2014 UKACC International Conference on Control (CONTROL)*, IEEE, New York, July 2014, pp. 104–109. https://doi.org/10.1109/CONTROL.2014.6915123

[50] Cook, A., *European Air Traffic Management: Principles, Practice and Research*, 1st ed., Ashgate, Farnham, England, U.K., 2007, pp. 166–168.

[51] Kent, T. E., and Richards, A. G., "On Optimal Routing for Commercial Formation Flight," *AIAA Guidance, Navigation, and Control (GNC) Conference*, AIAA Paper 2013-4889, 2013. https://doi.org/10.2514/6.2013-4889

[52] *Flight Schedules* (online database), OAG Aviation Worldwide, Luton, England, U.K., 2011, https://www.oag.com/airline-schedules-data [retrieved 1 Sept. 2011].

[53] de Wit, J. G., and Zuidberg, J., "The Growth Limits of the Low Cost Carrier Model," *Journal of Air Transport Management*, Vol. 21, July 2012, pp. 17–23. https://doi.org/10.1016/j.jairtraman.2011.12.013

[54] *FlightStats* (online database), Cirium, Portland, OR, 2014, https://www.flightstats.com [retrieved 7 Sept. 2014].

[55] Burghouwt, G., Hakfoort, J., and van Eck, J. R., "The Spatial Configuration of Airline Networks in Europe," *Journal of Air Transport Management*, Vol. 9, No. 5, 2003, pp. 309–323. https://doi.org/10.1016/S0969-6997(03)00039-5

[56] Prather, M. J., Wesoky, H. L., Miake-Lye, R. C., Douglass, A. R., Turco, R. P., Wuebbles, D. J., Ko, M. K. W., and Schmeltekopf, A. L., "The Atmospheric Effects of Stratospheric Aircraft: A First Program Report," NASA TR RP-127, 1992.

[57] Jet Fuel Price Monitor (online database), IATA, Montreal, 2020, https://www.iata.org/en/publications/economics/fuel-monitor [retrieved 7 Sept. 2014].